Academic Journal of Science and Technology
ISSN: 2771-3032 | Vol. 8, No. 3, 2023

Simulation of Supercritical Water Gasification Reaction of Glycerol and Reactor Structure Study

Jiarong Yin[1, a], Jinbiao Wang[1]

[1]School of Mechanical Engineering, Xi'an ShiYou University, Xi'an, Shaanxi, 710065, China
[a]jryin@xsyu.edu.cn

Abstract: The study established a reactor model with a volume of 500 ml that can withstand high temperature and high pressure, and firstly used the simulation software ANSYS FLUENT 2023R1 to simulate the process of generating H2-rich gaseous products by reacting glycerol in supercritical water at a temperature of 374°C and a pressure of 23 Mpa, and the results showed that the pressure and temperature were uniformly distributed in the fluid domain of the reactor. The results show that the pressure and temperature are uniformly distributed in the fluid domain of the reactor. Secondly, according to the pressure distribution obtained from the simulated reaction, the transient dynamics and thermo-mechanical coupling field analysis were applied to the inner wall of the reactor cavity in ANSYS Workbench to study the stress displacement. Finally, the results of the two analyses are compared to conclude that the pressure field can affect the trend of stress and displacement of the reactor structure, and the temperature field at higher temperatures can increase the values of stress and displacement.

Keywords: Supercritical water gasification; Reaction simulation; Reactor structure; Transient kinetic simulation; Thermo-mechanical coupled field analysis.

1. Introduction

Glycerol, as an important organic chemical raw material, has various uses in China. Its gasification reaction with supercritical water to generate green energy is also well studied. In this study, the reaction of glycerol in supercritical water is studied as a typical supercritical water gasification reaction to investigate its pressure field, temperature field and flow field.

Jin[1] and others established the kinetic model and computational fluid dynamics of the reaction between glycerol and supercritical water, simulated and analyzed the flow field, temperature, and chemical composition of the reactants and particle forms inside the supercritical reactor, and theoretically explained the reason for the generation of compounds that are difficult to decompose and easy to be deposited.Yao[2] and others combined the heat transfer of the reaction between biomass and supercritical water, chemical reaction, two-fluid model, and particulate flow dynamics to analyze the flow field of the reactor. Combining the flow field, residence time and temperature of the reactor on the gas production, they analyzed the effect of the flow field, residence time and temperature of the reactor on the gas production, and realized the improvement of the gas production rate.Guo[3] et al. established a kinetic model of the reaction between glycerol and supercritical water, and analyzed the liquid-phase products generated by the reaction, and finally proposed a simplified reaction route. Jia Chong[4] et al. determined the optimal process parameters for the supercritical water gasification of glycerol by experimental comparison and clarified the main consumption path of the reaction products. Wei Liping[5] et al. combined the multiphase flow of the reaction between biomass and supercritical water with particle flow dynamics, analyzed the effects of operating parameters such as flow rate and temperature on the flow characteristics, and obtained the particle distribution characteristics and the minimum fluidization velocity in the reactor.

Li Na[6] optimized the design of supercritical water oxidation reactor shell from the theoretical aspects of related literature, and determined the size ratio and strength constraints of the reactor. Gao Jun[7] and others used ANSYS analysis software to analyze the flange connectors of the supercritical water oxidizer for stress analysis under both pre-tensioning and operation, and obtained the stress distribution and deformation of each part. Li Zhenya[8] et al. determined the stress distribution and proposed an optimization method for the T-type impeller root wheel groove for a 10MW supercritical carbon dioxide turbine unit, and carried out stress analysis on the supercritical components. In addition to this there are many studies conducted on similar or related aspects, but there are fewer studies on the application of ANSYS FLUENT to clarify the temperature field and pressure field of the reaction process from the point of view of the simulation of the supercritical water gasification reaction, and on the basis of which the pressure distribution is applied to the inner wall of the fluid domain of the reactor to study the structural stress-strain distribution condition of the reactor, therefore, in this study, the stress distribution condition of glycerol in the interstitial fluid domain was simulated in ANSYS FLUENT software. Therefore, in this study, the pressure and temperature fields of the supercritical water gasification reaction of glycerol in a batch reactor were simulated in ANSYS FLUENT software, and on this basis, the stress-strain distribution was applied to the inner wall of the reactor to study the stress-strain distribution, which is expected to bring some references for the subsequent researchers.

2. Reaction Modeling

Supercritical water gasification reactor is the key equipment for hydrogen production by gasification of glycerin and supercritical water, which needs to be able to withstand high temperature and pressure and anti-corrosion function during the reaction process, so Hastelloy C-276 is

chosen.

2.1. Diameter and height of the internal chamber of the reactor

The reactor height to diameter ratio i=2 was determined based on the material type of the reactants containing oil sludge and water[9]. The internal diameter $D = \sqrt[3]{\frac{4v}{\pi i}}$, the internal height of the reactor $L=iD$, was calculated as D=69mm and L=138mm[10].

2.2. Reactor structure

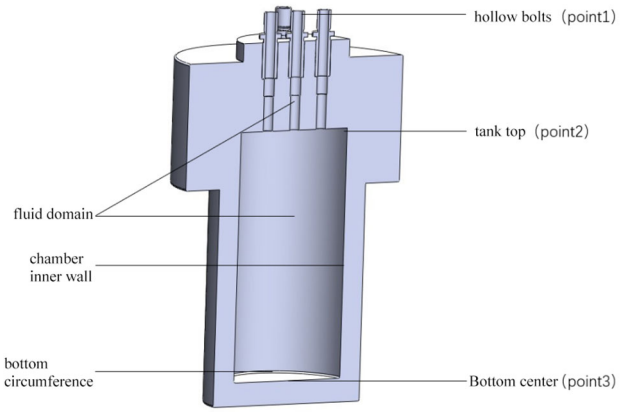

Figure 1. Sectional view of the reactor

The five hollow bolts on the top of the reactor were used as the inlet, outlet, upper temperature measurement port, lower temperature measurement port and pressure measurement port, and in addition, in order to minimize the bolted connection at the kettle lid and kettle body connection due to the coupling generated by the high temperature and high pressure, the kettle lid and the kettle body were regarded as an integral whole[11]. In the process of simulating the reaction, the pressure detection points were set up in the outlet at the top of the kettle, inside the kettle cavity and at the bottom of the kettle, and the internal pressure and temperature changes of the kettle during the reaction were analyzed representatively according to the calculation results of the points (node average value).

2.3. Mesh Division

The model is meshed using hexahedral structured meshing to remove the metallic structure of the reactor and retain the fluid domain. The mesh is encrypted at the contact between the hollow bolts and the fluid domain of the reactor and at the contact between the upper and lower planes of the reactor and the side walls[12].

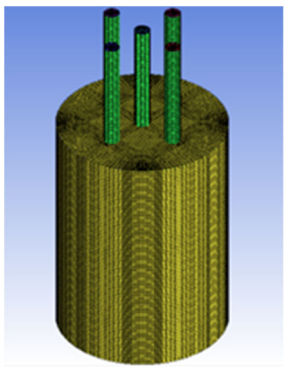

Figure 2. Fluid domain meshing

3. Supercritical Water Gasification Reaction Simulation

3.1. Verification of Grid Independence

Because this simulation achieves the effect of pressurization inside the reactor to 23Mpa by heating the reactor to generate water vapor inside after the reactor is filled with inert gases argon, glycerol and water. So after the start of the reaction should be carried out to seal the reactor[13], the internal flow and velocity is very small. Therefore low Reynolds number range is selected. In the case of low Reynolds number for simulating the reaction for the computational model k- , the mesh requires the dimensionless first layer of the adjacent wall distance y+ is taken as 1[14].

The total number of grids 233805, 451485, 688842, 971802 are generated for grid-independent calculations to study the effect of different total number of grids and local grid encryption on the simulated computational pressure results for the same y+ case. The simulation results are shown in Fig:

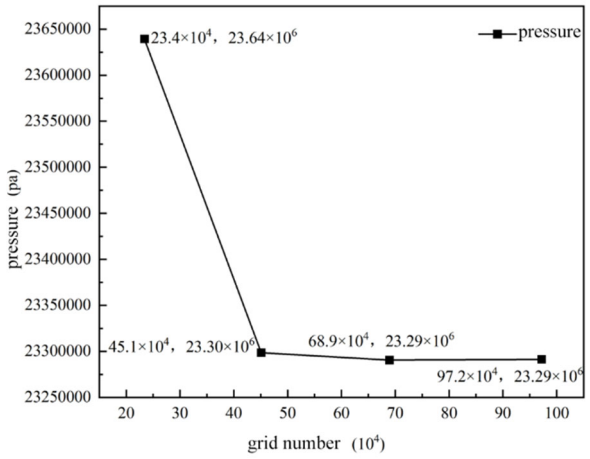

Figure 3. Grid-independence verification-pressure

Figure 3 is the global pressure inside the reactor, it is obvious that when the total number of grids is increased to 45.1×10^4, the simulated pressure inside the reactor cavity reaches 23.30Mpa and the change of the pressure starts to level off. Considering the calculation time and accuracy, the grid number of 45.1×10^4 is chosen for this simulation.

3.2. Software settings

Argon is an inert gas, and its physical properties remain stable at high temperature and pressure, so in order to pressurize to about 23Mpa, 80% by volume of argon, 15% water and 5% glycerol were injected into the reactor kettle cavity in advance[15]. The specific heat, thermal conductivity and viscosity of the supercritical water physical properties from 374°C to 382°C at 23.30Mpa obtained from the review of the data were input through segmented functions within the FLUENT material setup. In this simulation, the reaction temperature was started from 374°C, the reaction pressure was started from 23Mpa, the reaction residence time was ten seconds, and hydrogen, methane, carbon dioxide and carbon monoxide were generated, the reaction process was simulated using ANSYS FLUENT software to study the pressure and temperature fields in the reactor kettle cavity.

3.2.1. Reaction modeling

Treating argon, reactants and products as a mixture

homogeneous fluid, the reaction process involves energy conversion and requires the energy equation to be opened. The k-ω SST model is chosen, which is a computational model that is a hybrid of the k-ω model and the k-ε model, using a blending function (blending function) to achieve a gradual transition of the model from the standard k-ω model, which applies to the interior of the boundary layer, to the k-ε model, which applies to the exterior of the boundary layer and has a high Reynolds number.

3.2.2. Component equations

Component transfer model and volumetric reaction were chosen for the reaction model of glycerol with supercritical water. The actual reaction process is too complex it is difficult to quantitatively describe the reaction intermediates, so the set parameter method was used to describe it[16]. The ideal kinetic model of the reaction without considering coke and tar generation is expressed as follows:

Reaction 1. Glycerol pyrolysis I:

$$C_3H_8O_3 \xrightarrow{K_1} Int + CO_2 + 2H_2, R_1 = K_1 C_{C_3H_8O_3} \quad (1)$$

Reaction 2. Glycerol pyrolysis II:

$$C_3H_8O_3 \xrightarrow{K_2} Int + C0 + H_2 + H_2O,\ R_2 = K_2 C_{C_3H_8O_3} \quad (2)$$

Reaction 3. Intermediates steam reforming I:

$$Int + H_2O \xrightarrow{K_3} 2CO + 3H_2,\ R_3 = K_3 C_{Int} C_{H_2O} \quad (3)$$

Reaction 4. Intermediates steam reforming II:

$$Int + 3H_2O \xrightarrow{K_4} 2CO_2 + 5H_2,\ R_4 = K_4 C_{Int} C_{H_2O} \quad (4)$$

Reaction 5. Intermediate products pyrolysis:

$$Int \xrightarrow{K_5} CO + CH_4,\ R_5 = K_5 C_{Int} \quad (5)$$

Reaction 6. Water–gas shift reaction (WGSR):

$$CO + H_2O \xrightarrow{K_6} CO_2 + H_2,\ R_6 = K_6 C_{CO} C_{H_2O} \quad (6)$$

Reaction 7. Methanation:

$$CO + 3H_2 \xrightarrow{K_7} CH_4 + H_2O,\ R_7 = K_7 C_{CO} C_{H_2} \quad (7)$$

Where Int represents the intermediate, K_i represents the rate constant of the reaction, R_i represents the reaction rate of the reaction and C_i represents the concentration of each substance. Other aspects of the component equations were modeled using the component transfer model, volumetric reaction and diffusion energy source terms. For chemical reaction equation setup within the ANSYS FLUENT software, the simplified kinetic model uses all reactant and product leveling equations.

$$\ln k = \ln A - \frac{Ea}{R}\frac{1}{T} \quad (8)$$

Where the reaction activation energy Ea and the pre-exponential factor A are determined based on the K5 of the intermediate pyrolysis product of the fifth step of the kinetic model selected by the method of selecting the control step [3]. Because the value of K5 is the largest in the whole kinetic model, which indicates that the reaction rate of the fifth step of the reaction is the slowest, i.e., this step is the control step of the reaction rate. And Ea and A were determined according to equation (8).

3.2.3. Boundary conditions

The internal heat flux in the fluid domain of the reactor was set to 6000 W/m2·°C within the ANSYS FLUENT software.

3.2.4. Solution method setup

A pressure-based solver is used, the pressure solver is suitable for low velocity and incompressible fluids, in addition the pressure-velocity coupling method uses the coupled algorithm. In order to obtain more accurate data and better convergence of the residuals, the pressure is used in PRESTO!, the volume fraction is used in Geo-Reconstruct mode, and the turbulent kinetic energy and turbulent dissipation rate are used in the first-order windward algorithm.

3.3. Results and Discussions

3.3.1. Temperature distribution

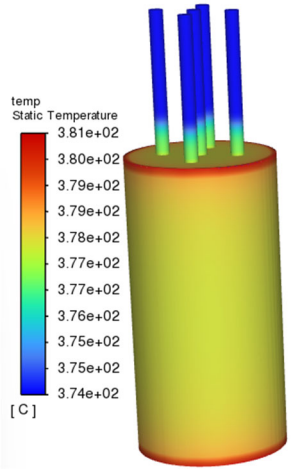

Figure 4. Temperature distribution in the fluid domain

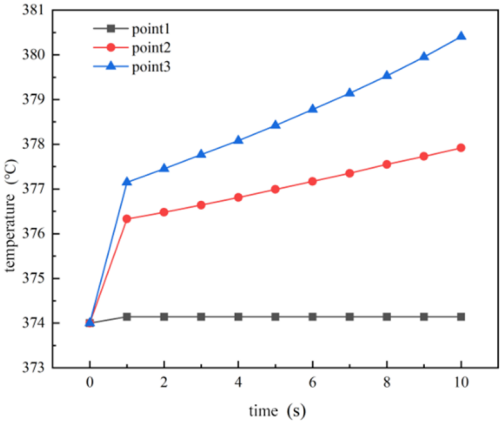

Figure 5. Temperature of the reactor

In Fig. 5 point1 is a nodal average of the upper end of the hollow bolt at the top of the reactor, point2 is a nodal average of the center of the circle at the bottom of the reactor, and point3 is a nodal average of the side wall of the reactor chamber in contact with the top. The meaning of nodal average is the average of the values of the grid center points in the smallest cell of the specified part of the grid added together and divided by the number of center points. The highest temperature after the completion of the reaction was at the kettle chamber side wall in contact with the top, with 380.4°C. The remaining parts of the temperature showed a slow increase during the reaction.

3.3.2. Pressure distribution

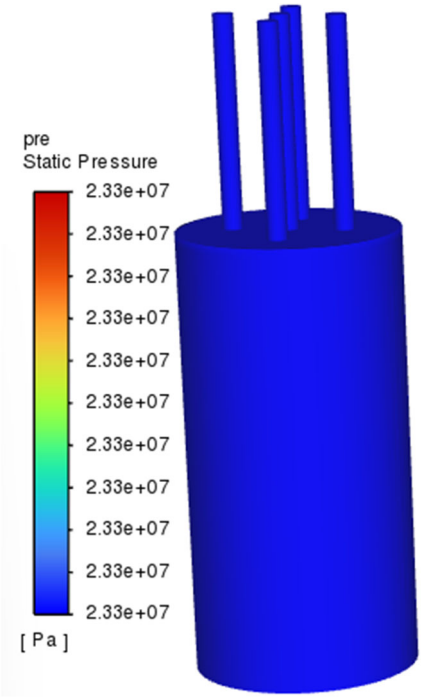

Figure 6. Fluid domain pressure distribution

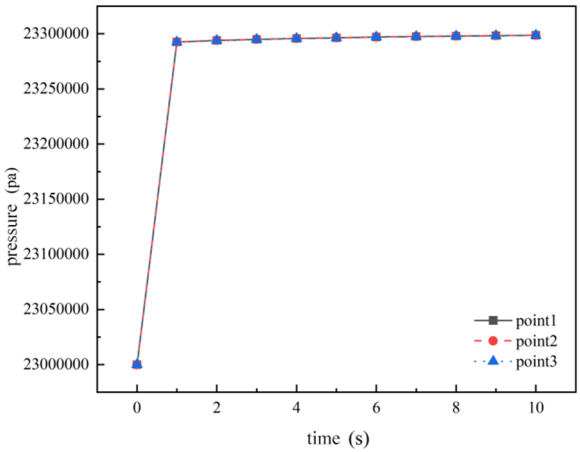

Figure 7. Pressure situation of the reactor

As shown in Fig. 6, the pressure in the fluid domain is also basically stable. Fig. 7 shows that the pressure at the beginning of the reaction stage rises rapidly to 23.29 Mpa in the first second, and slowly rises to 23.30 Mpa in the second nine seconds, because there is a volume fraction of 80% of argon gas filled with kettle cavity, so the pressure change in any place inside will be averaged to each part of the fluid domain, that is, the pressure and pressure change in any place inside the reactor kettle cavity are the same.

3.3.3. Changes in products with reaction time

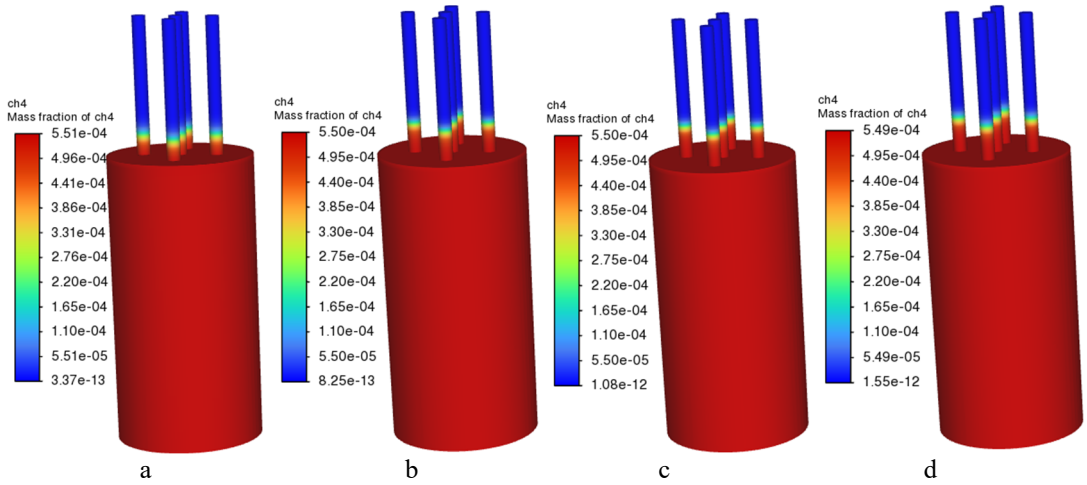

Figure 8. Variation of CH4 mass fraction with reaction time
(a: reaction time 0.5s, b: reaction time 2.5s, c: reaction time 5s, d: reaction time 10s)

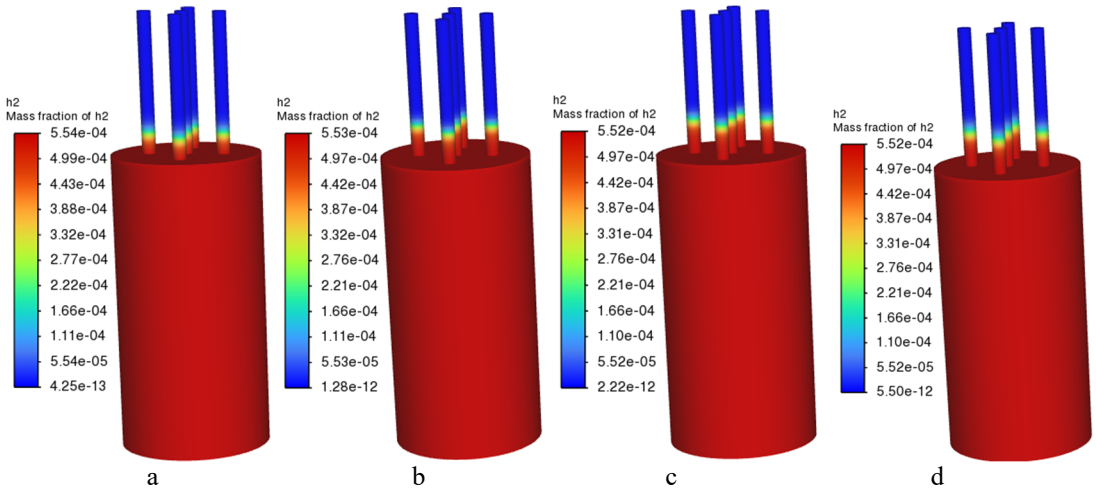

Figure 9. Variation of H2 mass fraction with reaction time
(a: reaction time 0.5s, b: reaction time 2.5s, c: reaction time 5s, d: reaction time 10s)

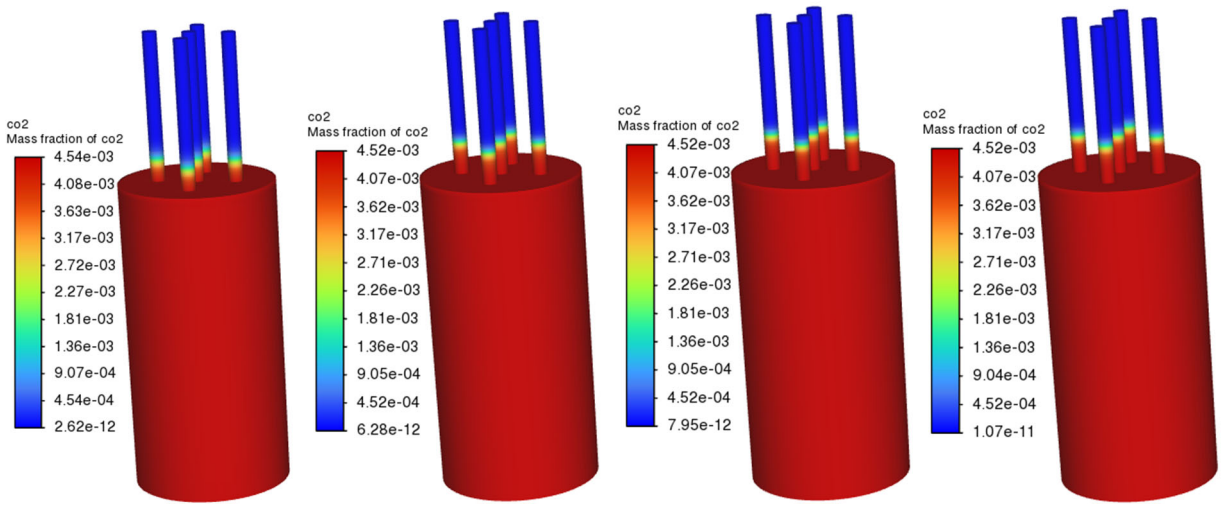

a b c d

Figure 10. Variation of CO2 mass fraction with reaction time
(a: reaction time 0.5s, b: reaction time 2.5s, c: reaction time 5s, d: reaction time 10s)

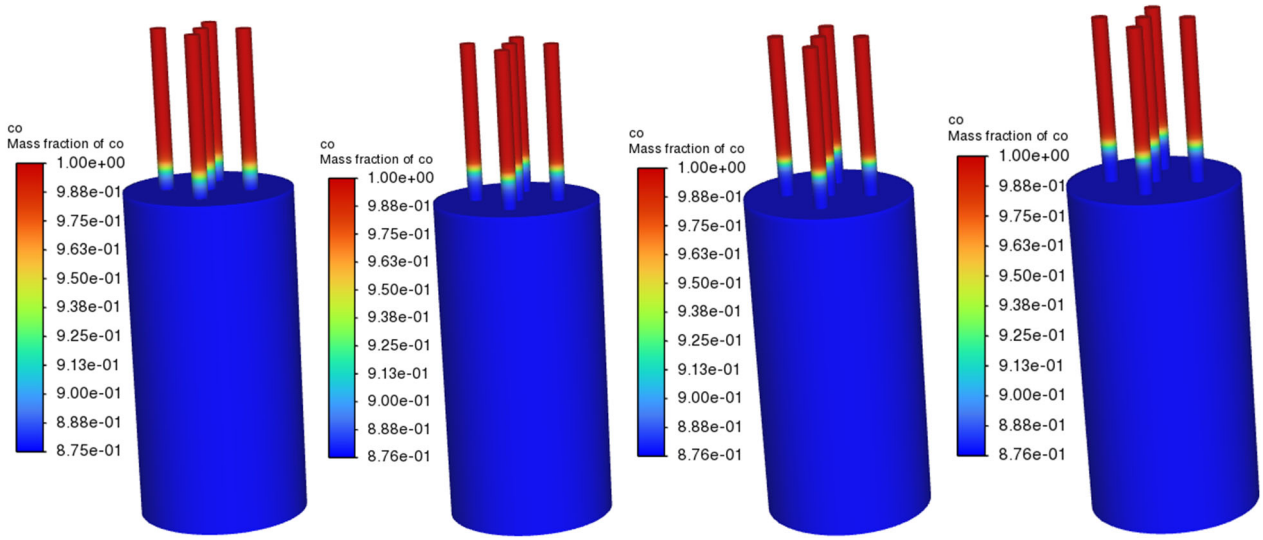

a b c d

Figure 11. Variation of CO mass fraction with reaction time
(a: reaction time 0.5s, b: reaction time 2.5s, c: reaction time 5s, d: reaction time 10s)

The distribution and variation of the products methane, hydrogen, carbon dioxide and carbon monoxide show that the reaction proceeded uniformly within the kettle area. The carbon monoxide mass fraction was highest at 100% inside the hollow bolt, and the highest mass fractions of the remaining three products up to the tenth second of the reaction were all inside the kettle cavity, 0.452% for carbon dioxide, 0.0552% for hydrogen, and 0.0549% for methane. According to the product distribution graph, the reaction stabilized around 2.5 seconds. The mass fractions of the products carbon dioxide, hydrogen, and methane can be seen slowly spreading up the hollow bolt as the reaction proceeds, indicating that the reaction is producing the corresponding gases. Carbon monoxide is also consumed as the reaction proceeds to produce the rest of the products, so the unconsumed portion of the carbon monoxide can be seen to collect mainly in the hollow bolt from Figure 11.

4. Reactor Structure Simulation Study

The transient dynamics and steady state thermal-mechanical coupling field of the reactor structure are investigated from two perspectives, and the final calculation results are compared to derive the way the temperature field and pressure field affect the reactor structure.

4.1. Transient dynamics analysis

The model is imported into ANSYS Workbench, and the constraints of x, y, and z are added to the imprinted surface for constraints at the connection between the kettle lid and the kettle body and at the outside of the kettle cavity with the displacement of 0 in each direction, in order to simulate the ferrules used for fixing the kettle at the above two parts of the kettle in the real experimental reaction situation. A simulated pressure field is added to the inside of the reactor chamber for a total of ten seconds, divided into the first second of the faster pressure rise and the last nine seconds of the slower rise. After the operation was completed, calculations were started to produce stress and strain diagrams for the reactor.

4.1.1. Dynamical stress distribution results and discussion

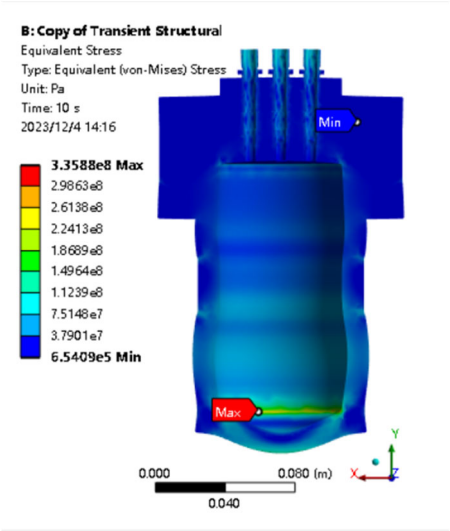

Figure 12. Stress profile of the kinetics reactor

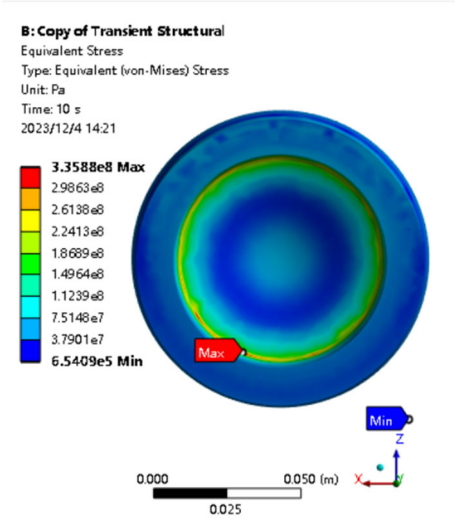

Figure 13. Dynamics reactor bottom stress

As shown in Figure 12, the maximum stress and minimum stress in the bottom of the reactor kettle circumference and kettle kettle cover connection, Hastelloy c276 in 300 ~ 800 ℃ within the minimum tensile strength of 600Mpa, the figure of the maximum stress value of 335.9Mpa in line with the stress requirements of Hastelloy c276.

4.1.2. Results and Discussion of Kinetic Displacement Distribution

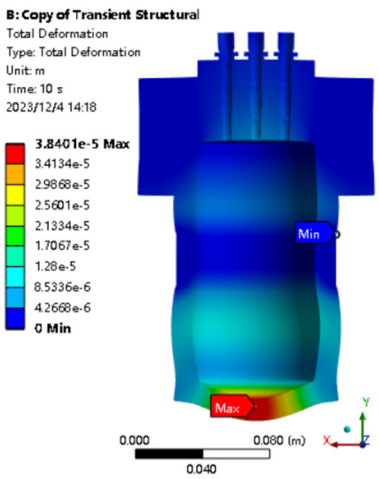

Figure 14. Kinetics reactor displacement profile

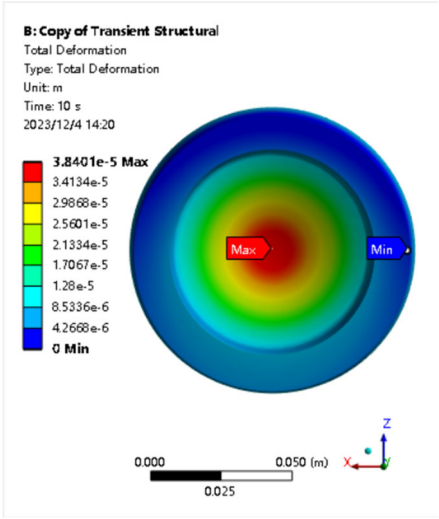

Figure 15. Dynamics reactor bottom displacement

From Fig. 15, the largest displacement occurred in the bottom center of the kettle in the negative direction of the y-axis, with a displacement value of 0.038401 mm. The rest of the displacement occurred mainly around the imprinted surface of the added constraints, with different degrees of outward expansion of the displacement, including the inner cavity of the reactor kettle and the contact of the hollow bolts. It can be assumed that these displacements are caused by the outward pressure inside the reactor cavity where the reaction occurs, and the extent of the displacements may be even greater if the influence of the temperature field on the reactor is taken into account.

4.2. Thermo-mechanical coupling field analysis

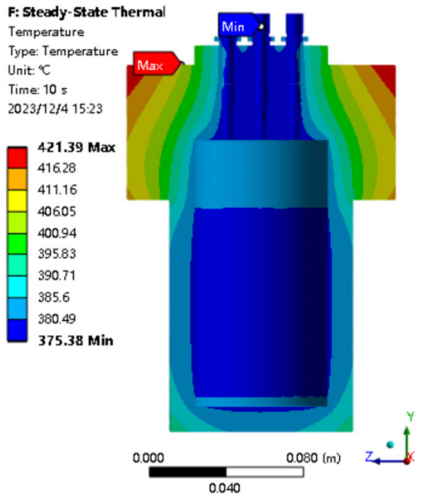

Figure 16. Steady-state thermal reactor temperature distribution

Thermo-mechanical coupled field analysis in the consideration of pressure at the same time, but also the high temperature on the reactor structure was analyzed, after comparison with the results of the transient dynamics analysis can be derived from the temperature field and pressure field for the reactor structure of the influence of the way.

The model is imported in ANSYS Workbench and the steady state heat load calculation is performed first. Add Nickel alloy,Hastelloy C-276 as the reactor structure material inside the application, set up two kinds of convection inside and outside the reactor, and then set up the heat flux of the

overall structure of the reactor, which are all three conditions for the steady state fixed numerical heat load. The temperature distribution inside the reactor structure is summarized in Fig. 16. Among them, the highest temperature on the upper side of the kettle lid reaches 421.39℃, and the lowest temperature inside the kettle cavity is 375.38℃. Secondly, the kinetic-mechanical analysis coupled with the thermal loads was performed to obtain the results of the coupled-field analysis after adding the pressure to the sub-parts and other operations.

4.2.1. Coupling field stress distribution results and discussion

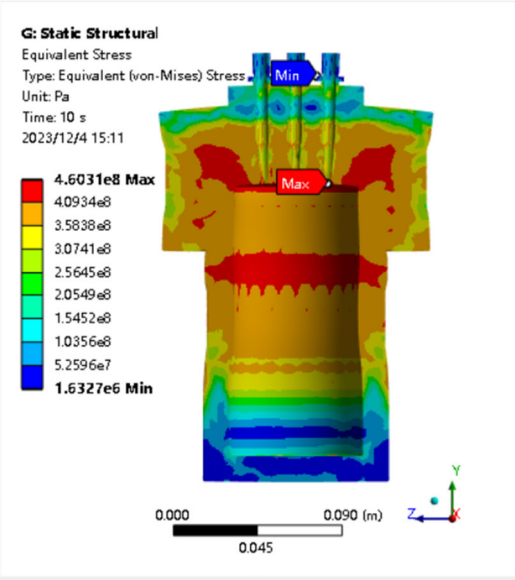

Figure 17. Coupled-field reactor stress profile

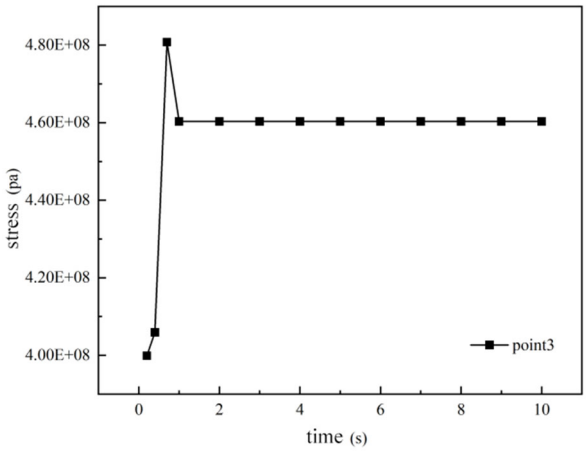

Figure18. Stress variation at the upper end of the kettle cavity

Fig. 17 The maximum stress is 460.3 MPa at the upper end of the kettle cavity because of the structural discontinuity of the kettle at this point. The minimum stress is 163.3 MPa at the top of the hollow bolt, considering the connection between the kettle body and kettle cover, the maximum stress may lead to the damage of the kettle. The stress in the middle of the reactor kettle cavity has the same magnitude as the stress at the top, which may be due to the outer constraints that make it more stressful during the reaction process. Figure 18 shows the stress change of point3 during the ten seconds of the simulated reaction, after a brief increase to 480.8 MPa it remained at 460.3 MPa from the first second.

4.2.2. Coupled Field Displacement Distribution Results and Discussion

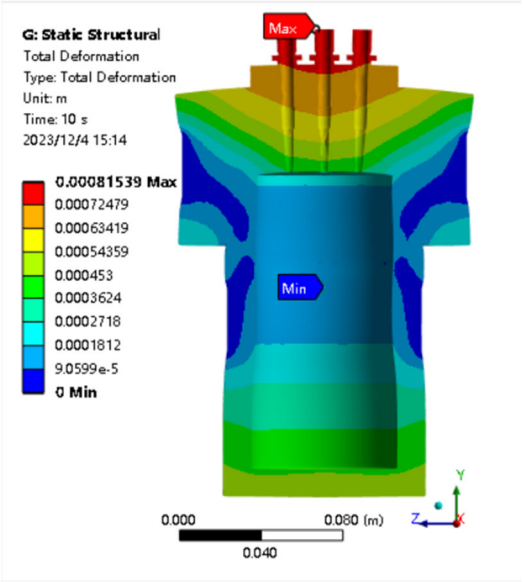

Figure 19. Coupled-field reactor displacement profile

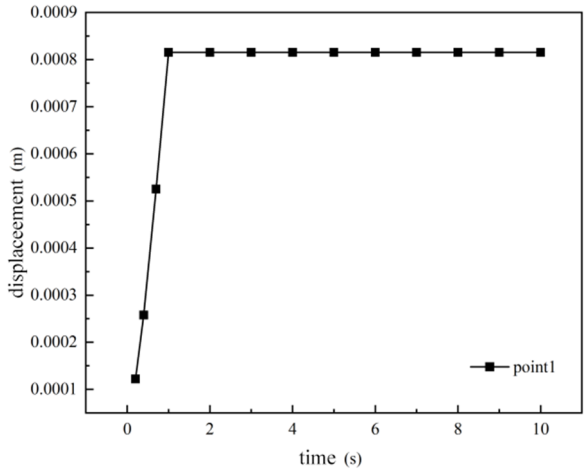

Figure 20. Variation of displacement in the upper part of the hollow bolt

Figure 19 The maximum displacement occurs in the upper part of the five hollow bolts to reach 0.81539mm, and the minimum displacement of 0 is mainly concentrated in the vicinity of the two constraints. The maximum displacement of the upper part of the hollow bolts is due to the fact that the reactor has the largest structural change at that place, and the hollow bolts are mechanically connected to the reactor. Figure 20 shows the displacement change of point1 in ten seconds of simulated reaction time, which is finally fixed at 0.81539mm after one second of increase.

After the comparison of Fig. 18 and Fig. 20 with Fig. 7, it can be seen that the pressure change in the simulated reaction within 10 s is concentrated in the first second of the reaction, and in the subsequent coupled-field analysis, the pressure is applied to the kettle cavity, which ultimately also causes the stress and displacement to keep the constant value after increasing in the first second of the reaction. Comparison of the stress and displacement values with those of the kinetics reveals that the stress and displacement values of the coupled field have a wider range, with the maximum value even reaching about 20 times of the maximum value of the kinetics. With the same loading pressure in the kinetic and coupled fields, it is believed that the main reason for the increase in

the values of stresses and displacements is the temperature field at higher temperatures.

5. Conclusion

In this study, the simulation of the gasification reaction of glycerol in supercritical water was carried out to derive its pressure and temperature fields, and finally the pressure distribution was applied to the inner wall of the reactor to study its stress-strain distribution. Based on the results, the following conclusions were obtained:

(1) The inert gas argon for internal pressurization and the rest of the compounds involved in the reaction were set up as multiphase flows. The viscous model is chosen as the k-ω SST model that meets the low Reynolds number requirement. The coupled algorithm is chosen for the coupling method. The pressure and temperature fields are relatively stable during the simulation, and combined with the distribution of the products in the reactor both indicate that the reaction is uniformly distributed in the reactor.

(2) The stress and displacement changes obtained from the thermal-mechanical coupled field analysis are consistent with the pressure changes obtained from the simulated reaction, indicating that the applied pressure affects the trend of stress and displacement. Transient dynamics and thermal-mechanical coupling field for the reactor structure stress, displacement analysis results are not the same, but after comparison can be seen in the coupled field stress, displacement values in all parts of the reactor are greater than the transient dynamics analysis of the stress, displacement values, indicating that the high temperature of the temperature field can make the reactor structure stress, displacement values increase.

Acknowledgment

Funds: Shaanxi Provincial Natural Science Basic Research Program: Research on the reaction mechanism of petroleum hydrocarbon pollutants in the NSCWG reaction of oil-bearing drilling solid waste. (2022JQ-550).

References

[1] JIN Hui,GUO Simao,Guo Liejin,et al.A mathematical model and numerical investigation for glycerol gasification in supercritical water with a tubular reactor [J]. Journal of Supercritical Fluids, 2016, 107:526-533.

[2] YAO Liang,LU Youjun.Supercritical water gasification of glucose in fluidized bed reactor:A numerical study [J]. International Joumal of Hydrogen Energy, 2017, 42(12): 7857-7865.

[3] GUO Simao,GUO Liejin,YIN Jiarong,JIN Hui. Supercritical water gasification of glycerol: Intermediates and kinetics [J]. The Journal of Supercritical Fluids,2013,78:95-102.

[4] JIA Chong,GUO Xin,ZHEN Senlin,et al. Process parameters and kinetics of hydrogen production from supercritical water gasification of glycerol[J]. Journal of Southwest Forestry University, 2023, 43(5):135-144.

[5] WEI Liping,LV Youjun,GUO Liejin. Numerical simulation study of two-phase flow characteristics in a supercritical water fluidized bed [J]. Journal of Engineering Thermophysics, 2011, 32(5):803-806.

[6] LI Na,ZHAO Guangming. Optimization of supercritical water oxidation reactor shell design[J]. Shandong Chemical Industry, 2020, 49(4): 165-166.

[7] GAO Jun, SHAN Yuhai, ZHANG Jianmin,at al. Finite element analysis of bolted flange connectors for supercritical water oxidation reactors [J]. Mechanical Engineering&Automation, 2014, 186(5):34-38.

[8] LI Zhenya,ZHAO Fneg,ZHU Youjun,FAN Xuefei.Optimized design of supercritical carbon dioxide turbine impeller root groove structure[J]. Journal of Chinese Society of Power Engineering, 2021, 41(5):640-644.

[9] Dong Junhua,Gao Bingjun. Mechanical fundamentals of chemical equipment [M]. Beijing:Chemical Industry Press, 2019.

[10] GB/T 150.3-2011. Pressure vessels Part III: Design [S]. Beijing: AQSIQ,2011.

[11] DUAN Yuanwang. Experimental study of hydrogen production from supercritical water gasification of oil-containing sludge [D]. Xian: Xian Shiyou University,2020.

[12] LI Meng,TAO Leren,YU Zhongyang,YU Qing. Numerical study of supercritical CO2 cooling heat transfer in a horizontal spiral groove tube[J]. Journal of Engineering for Thermal Energy and Power,2021,36(4):51-59.

[13] WANG Zhi,WU Yuxiao,HAN Xu,CAI Wenkui,MENG Jin. Performance Analysis of Supercritical CO2 Combined Dry Gas Seal[J]. Journal of Chinese Society of Power Engineering, 2023，43(9):1143-1150.

[14] Ji Bingbing,Chen Jinbao.ANSYS ICEM CFD meshing technology example explanation[M]. Beijing:China Water Resources and Hydropower Press, 2011.

[15] LIU Xuebin. Study on the mechanism of hydrogen production from supercritical water gasification of oil-containing sludge under alkaline catalytic conditions[D].Xian:Xian Shiyou University,2021.

[16] OU Guobiao,REN Yifei,JIN Hui,et al. Kinetic modeling of supercritical water gasification of typical coal types[J].Journal of Engineering Thermophysics,2022,43(8):2009-2018.